International Journal of Applied Engineering Research ISSN 0973-4562 Volume 10, Number 14 (2015) pp 34501-34508

Harvesting vertical vibration of automotive tyre to monitor tyre pressure using applied machine learning technique

[1]Hemanth Mithun Praveen, [2]V. Sugumaran
[1,2]School of mechanical and building science, VIT University Chennai campus, Chennai, India
[1]hemanth.mithun.praveen@gmail.com, [2]v_sugu@yahoo.com

Abstract- Tyre pressure monitoring systems are automotive systems which monitor tyre pressure in real-time. Most systems depend on barometric pressure sensors to measure tyre pressure and transmitters to send data toward the receiver. These sensors have to be placed between the tyre and the rim which exposes them to harsh mechanical conditions; extreme temperature and mechanical shocks. This paper proposes a new indirect method to monitor the tyre pressure by harvesting the vertical vibrations from the wheel hub of a running vehicle. The problem will be treated as a fault diagnosis problem. The vibration signals would then be represented as histogram features. The acquired histogram features would be classified using support vector machine algorithms to acquire the best classification accuracy there by determining the best algorithm.

Keywords- Tyre pressure monitoring systems, Fault diagnosis, Support vector machine, Accelerometer, Machine learning.

1. Introduction

Puncture is a common event associated with pneumatic tyres. No matter how well maintained, a puncture may occur on an average of 40233.6 km [1]. Tyres may or may not depend on pressurised air to maintain their shape. They can be broadly classified as pneumatic and non pneumatic tyres. For automotive applications the tyre used is of the pneumatic category. The pneumatic tyres can differ by construction. Simple pneumatic tyres such as bicycle tyres are constructed using a belt/ply type construction. Diagonal tyres are used for rough surfaces as their sidewalls are much stronger than radial tyres. However, the driving comfort and heat dissipation of these types of tyres are below satisfactory as when compared to radial tyres. Radial tyres are the most commonly used type for automobiles as they provide good fuel economy, stability and comfort. Every tyre will be identified with a code which would be on the side walls of the tyre. The tyre chosen for this study was coded as 145/70 R12 69 T. Here '145' denotes the tyre width in millimetres, '70' denotes the tyre profile in millimetre, and 'R' denotes that the tyre construction type is a radial tyre. '12' denotes the rim size in inches. '69' is the load index value. It denotes the maximum load allowed for the tyre. Here '69' correspond to 325 kg. 'T' is the speed rating code and denotes the maximum safe speed of the tyre. Here 'T' corresponds to 190 km/hr.

Since tyres depend on pressurised air to maintain their shape monitoring tyre pressure is important to ensure the tyre operates at optimum performance. Tyre pressure monitoring systems are automotive sensor systems which are attached to the vehicle to report the tyre pressure on a real-time basis. They can broadly be classified as direct and indirect systems depending on their mode of operation and data acquisition [2].

Direct tyre pressure monitoring systems depend on barometric pressure sensors to 'read' the tyre pressure. This sensor with other electronic such as batteries, wireless data transceiver etc which are housed in a plastic case are strapped to the rim of the tyre or attached to the neck of the tyres. Since battery power is limited. The sensors enter a sleep mode to conserve power when not in use. They depend on a wake up circuit to reactivate and resume normal operation. Some modules relay on an impulse from a low frequency receiver which is transmitted from the main TPMS control unit. Other TPMS modules depend on an accelerometer to detect the centrifugal acceleration when the tyre starts to move from rest [3]. However, most TPMS sensors do not allow a battery replacement. If the battery can be replaced, replacing a battery requires separation of the tyre from the rim. Moreover each wheel requires a dedicated sensor (Figure 1) this will add up cost when additional wheels are used for snow tyres or off-road tyres. A common defect reported by direct TPMS users was that the valve stem would corrode and would break with the slightest amount of torque. Another drawback of direct TPMS is that it cannot be used in conjunction with self-sealing solvents as it clogs the port of the barometric pressure sensor, rendering the sensor non-operational until cleaning [4].

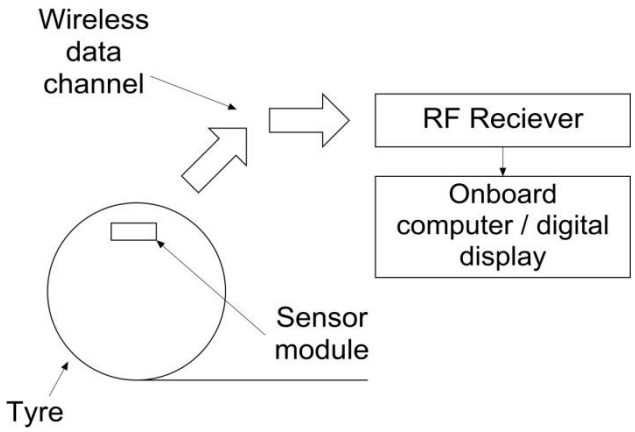

Fig 1 Direct TPMS

Indirect tyre pressure monitoring systems don't use pressure sensors. They depend on the wheel speed sensor used by the anti-lock breaking system to estimate the tyre pressure (Figure 2). An under inflated tyre would have a

slightly smaller wheel radius when compared to other tyres; there by inflicting a change of RPM. Since wheel speed is used to calculate the tyre pressure, these systems cannot display absolute pressure readings. They can only display relative data such as difference in wheel speed [5][6].

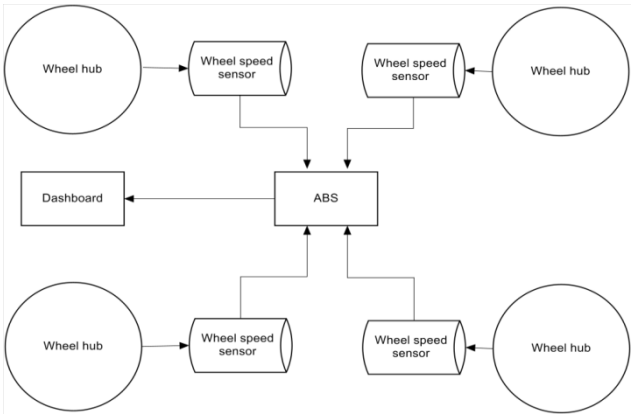

Fig 2 Indirect TPMS

Changzheng *et al.* (2012) developed a micro machined piezoresistive pressure sensor and self testable accelerometer for tyre pressure monitoring system. The author claims that the fabrication technique could completely integrate the sensing elements [3]. Zhou *et al.* (2012) carried out a research on algorithms for tyre pressure monitoring based on multiple sensor information fusion and Bayesian. It was concluded that the information sensor fusion was better than the Bayesian method [7]. Knawar *et al.* (2012) proposed a piezo electric vibration harvesting system (Figure 2.6). This system uses a sensor to generate electrical power from vibration harvested from a running tyre there by powering tyre pressure monitoring sensors [8]. Hamed *et al.* (2013) carried out a research on the influence of vehicle tyre pressure on suspension system. The response of the suspension system was analysed by applying the time – frequency approach. The vertical vibrations generated by the system were used for data analysis [9]. Carcaterran and Roveri (2013) investigate tyre grip identification based on strain information where the tyre road grip condition could be estimated from the strain information acquired from the tyre [10]. Dubois *et al. (2013)* conducted a study in which low frequency statistical estimations of rolling noise of tyre and road were calculated numerically [11]. Amarnath *et al.* (2013) presented an algorithm based interpretation of sound signals for automated evaluation of bearing condition. From acquired sound data, a model was built using data modelling technique. Decision tree (C4.5) algorithm was used to learn and classify the condition of the bearing [12]. Jegadeeshwaran *et al.* (2013) used C 4.5 decision tree algorithm and best first decision tree algorithm for classifying brake faults using the statistical features extracted from the vibration signals of a static brake test rig. The highest accuracy was reported to be 97.81 % [13]. Muralidharan *et al.* (2013 a) investigated vibration based fault diagnosis of mono block centrifugal pump. Wavelet analysis was used to extract a set of features. Classification using Naïve Bayes and Bayes net algorithm were carried out. The author concluded that feature extraction using wavelets as well as Bayes net algorithm for classification was found to be combination for practical applications of fault diagnosis of mono block centrifugal pump [14]. Muralidharan *et al.* (2013 b) investigated vibration based fault diagnosis of mono block centrifugal pump. The author concluded that feature extraction using wavelets, rule generation using rough set, and classification through fuzzy logic algorithm for classification was found to be combination for practical applications of fault diagnosis of mono block centrifugal pump [15].

From the above section it can be concluded that many methods were developed to measure the tyre pressure. Some methods used capacitive and resistive properties of the tyre while others used barometric pressure sensors and accelerometers. Since the problem was treated as a fault diagnosis problem further literature related to fault diagnosis was reviewed. However the contribution towards tyre pressure monitoring system for fault diagnosis approach was close to none. Hence this paper proposes a new indirect method to monitor the tyre pressure by extracting the histogram features from the vibration signals and classifying them using the support vector machine algorithm.

2. Experimental Setup

To conduct the experiment, a front wheel drive vehicle was chosen. Pressure readings were taken for different conditions; normal, puncture and idle. Tyre pressure readings of 28 psi were taken as normal and pressure readings of 22 psi and below were taken as puncture. The test speeds were limited from 20 km/hr to 80 km/hr. The speed of the vehicle was varied in a normal driving method. Speeds below 20 km/hr did not give sufficient amplitude hence they were classified as idle, irrespective of their tyre state. A tri-axial MEMS accelerometer was used to acquire the vibration data. Figure 3 represents the MEMS accelerometer module. Table 1 shows the accelerometer specifications. Figure 4 illustrates the axes of the accelerometer. Figure 5 represents the experimental setup. A total of 330 samples of 1000 data points each at a sampling rate of 66 Hz were taken. Equal numbers of samples were acquired for all three classes in order to ensure the experiment unbiased. The classes were titled as 'Normal', 'Puncture' and 'Idle'. A data acquisition system (Table 2 and Figure 6) and program (Figure 7) was developed for the study.

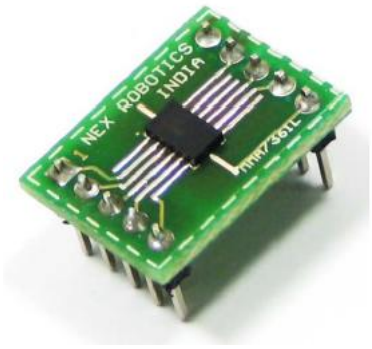

Figure 3 MEMS Accelerometer module

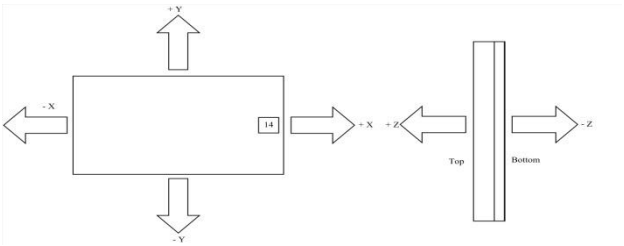

Figure 4 MEMS Accelerometer axis (From datasheet)

The accelerometer module was coated with a waterproof gum and fixed to the axel of the rear right wheel of the car (Figure 5). A shielded wire was used to minimize external electronic interference.

Figure 5 MEMS Accelerometer fixed on the axel

Table 1 MEMS accelerometer specification

FEATURES	SPECIFICATION
Make	Freescale Semiconductor
Weight	<1g (accelerometer only) 5g with supporting electronics
Type	MEMS
Number of Axis	3
Description	±1.5 g ±6 g Selectable range
Frequency	1 – 400 Hz (X and Y axis) 1 – 300 Hz (Z axis)
Resonance Frequency	6 kHz (X and Y axis) 3.4 kHz (Z axis)
Sensitivity	800 mV/g @ 1.5g 206 mV/g @ 6g
Connector	LGA-14 Package (SMD component)

Table 2 specification of DAQ system used for MEMS sensor

FEATURES	SPECIFICATION
Make	self
PC communication	USB/RS232
Number of input Channel	3
ADC Type	Successive approximation
ADC resolution	10 bit
Max sampling rate	15kHz

Figure 6 data acquisition system

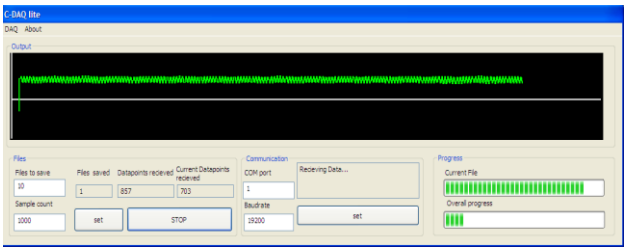

Figure 7data acquisition program

The sample waveform of the tyre's vibration from the MEMS sensor for the conditions of normal, puncture and idle are shown in Figure 8, 9, 10 respectively.

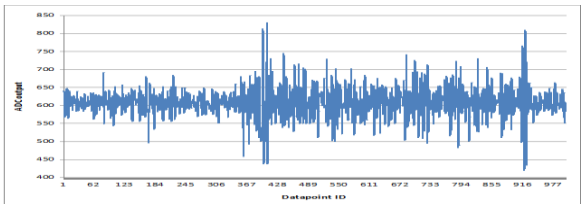

Figure 8 Sample signal of Normal condition from MEMS accelerometer

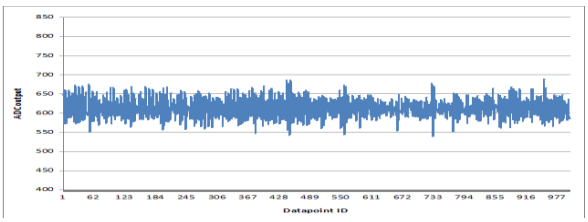

Figure 9 Sample signal of Puncture condition from MEMS accelerometer

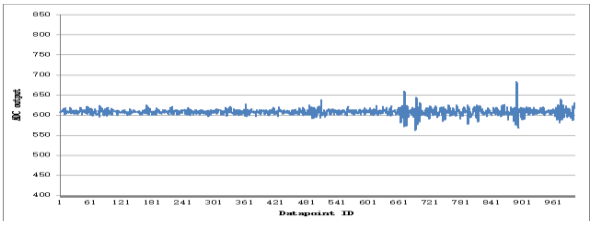

Figure 10 Sample signal of idle condition from MEMS accelerometer

2.1. Sampling Rate Calculation

The tyre used was 145/70 radial tyre with a max pressure rating of 44 psi.
Radius of tyre (R) = 25cm
Maximum Speed in km/hr (S) = 80km/hr (22.22 m/s)
Minimum Speed in km/hr (S) = 20km/hr (5.55 m/s)
Since the wheel radius and the speed in known RPM can be achieved by equating it to known variables (R, S)
Minimum RPM & Frequency
$2 \prod \times 0.25(R) \times RPM/60 = 5.55$
RPM =212
Frequency = 212/60 = 3.53 Hz
Maximum RPM & Frequency
$2 \prod \times 0.25(R) \times RPM/60 = 22.22$
RPM =848
Frequency = 848/60 = 14.13 Hz
According to Nyquist Shannon sampling theorem, the minimum sampling rate should be at least double the highest incoming frequency in order to avoid antialiasing effect [16].Hence the minimum sampling rate must be 28.26 Hz. The sampling rate was set at 66Hz.

3. Machine Learning

There are three phases in machine learning; Feature extraction, feature selection, feature classification. The vibration signal was used to extract the histogram features to yield the required parameters. The features were the designated inputs for the classifiers for the model building purpose.

A. Feature Extraction

Feature extraction is the process of extracting the features from the signal there by representing it as a string of values. Excel was used to compute the statistical features. Once a raw signal was obtained the histogram features were extracted from the signal. The process had to be repeated for 330 files for each bin size. Hence a macro was written to carry out the task.

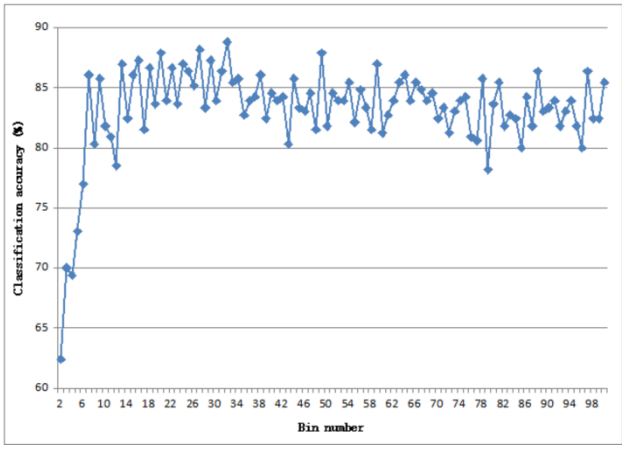

Figure11 Classification accuracy of different bin sizes with J48 classifier

The bin range was varied from 2 to 100 and the required features were extracted. Each bin was tested with the J48 algorithm and the classification accuracy was noted (Figure11). When varying the number of bins, classification accuracy was found to drop after a particular bin value. The bin numbers were stopped at 100 as the classification accuracy was dropping.

B. Feature Selection

Feature selection is the process of selecting the best contributing features acquired from the feature extraction process. The non-contributing features would be rejected to reduce computational load and improve the classification accuracy. In the case of histogram feature selection, the appropriate bin size must be selected first. Here, J48 classifier was used to undertake the task of feature selection as it gave the best accuracy. J48 is the 'java' implementation of the c4.5 algorithm [17]. J48 was also reported to perform well for studies related to fault diagnosis [18]. The decision tree generated by the classifier is shown in Figure12. All 99 bins were tested with the J48 classifier (Figure11). Out of which, bin number 32 yielded the maximum result of 88.18%. Hence bin number 32 was chosen for the feature selection process. From this process, the features selected from bin 32 were H9, H15, H16, H18, H19, H20, H21, H22, H24 and H25. These attributes were chosen from all the other features by the classifier. The remaining attributes were rejected [?].

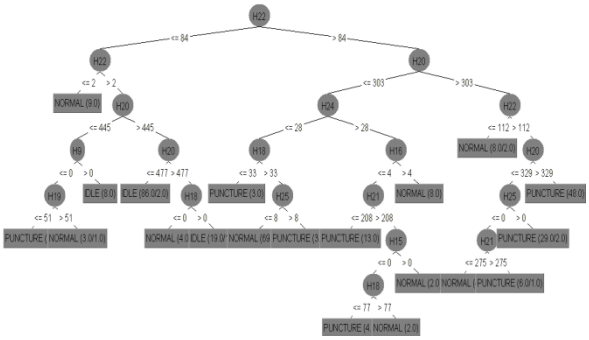

Figure12 Decision tree generated using the J48 tree algorithm

Total number of Leaves : 20
Total size of the tree : 39
Time taken to build model: 0.03 seconds

Table 3 Cross-validation for J48

TP	FP	PR	R	F	RO	C
0.8	0.059	0.871	0.8	0.834	0.875	**N**
0.864	0.091	0.826	0.864	0.844	0.886	**P**
1	0.018	0.965	1	0.982	0.988	**I**
0.888	0.056	0.887	0.888	0.887	0.917	**W**

TP stands for True Positive Rate, FP stands for False Positive Rate, PR stands for Precision, R stands for Recall, F stands for F Measure, RO stands for ROC area, C stands for Condition, N stands for Normal, P stands for Puncture, I stands for Idle, W stands for Weight average. Table3 shows the detailed accuracy by class for the untrained J48 classifier.

Table 4 shows the stratified cross-validation details for the untrained J48 classifier. Table5 shows the confusion matrix generated by the untrained J48 classifier. Table6 shows the parameters for the J48 classifier

Table4 Cross-validation for J48

Parameters	Results
Correctly Classified Instances	293/330
Kappa statistic	0.8318
Root mean squared error	0.2647
Root relative squared error	56.1433 %
Incorrectly Classified Instances	37/330
Mean absolute error	0.0888
Relative absolute error	19.9839 %
Total Number of Instances	330

Table5 Confusion matrix generated J48 tree

Classified as	Normal	puncture	Idle
Normal	88	20	2
Puncture	13	95	2
Idle	0	0	110

Table6 Values for objects of the trained J48 tree

Sl No.	Objects	Value
1	Confidence factor	0.25
2	Minimum number of objects	2
3	Number of folds	3
4	Seed	1

From the Figure11, it is clear that bin 32 had attained the maximum classification accuracy of 88.78%. 88/110 samples were correctly classified as normal, 95/110 samples were correctly classified as puncture, and 110/110 samples were correctly classified as idle. These could be noted as the diagonal elements in the confusion matrix tabulated in Table 5. This denotes the correctly classified classes. However, 13/110 samples that is 11.80 % of the class 'puncture' was incorrectly correctly classified as normal. Moreover 20/110 samples that is 18.18 % of the class 'Normal' were incorrectly correctly classified as puncture. Adding to the previous misclassification 2 samples of each of normal and puncture were misclassified as idle this was about 1.81% per class. This clearly indicates that a study is required in reducing misclassification there by increasing the classification accuracy.

C. Feature Classification

The Support Vector Machine (SVM) is a new generation learning system based on statistical learning theory. In classifying low dimensional non linear problems, often the classifier faces a lot of difficulty in classification. This problem is tackled in SVM. The idea is to map the original pattern space into the high dimensional feature space through some non-linear mapping functions, and then construct the optimal separating hyper plane in the feature space. Thus, the non-linear problem in low dimensional space corresponds to the linear problem in the high dimensional space. SVM comes under the category of supervised learning algorithms in which the learning machine is given a set of features with the associated labels (or output values). Each of these features can be looked upon as a dimension of a hyper-plane. SVMs construct a hyper-plane that separates the hyper-space into two classes (this can be extended to multi-class problems). While doing so, SVM algorithm tries to achieve maximum separation between the classes [19].

4. Results and Discussion

Two SVM kernels with four functions each were used to compute the result. The kernels were

1. C-SVC
2. nu – SVC

The functions were

1. Linear
2. Sigmoid
3. Polynomial (2nd degree)
4. RBF (Radial Basis Function)

A total of 10 features were selected by the feature selection process. These features were used for the feature classification process.

Table 7 and Figure 14 show the classification accuracy of different kernels with different functions. Figure 13 and Table 8 shows the processing time of different kernels with different functions.

Table 7 Classification accuracy of different kernels

Classification %	Linear	Polynomial	RBF	Sigmoid
C-SVC	83.94	86.97	92.12	83.94
nu-SVC	83.03	85.76	91.82	78.18

Table 8 Comparison of processing time for different kernels

Classification time	Linear	Polynomial	RBF	Sigmoid
C-SVC	9s	20m 3s	14s	3m 54s
nu-SVC	2s	5m 58s	7s	1m 30s

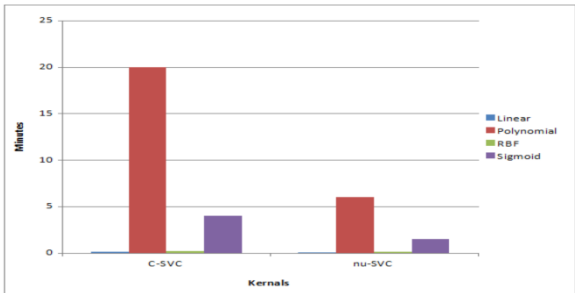

Figure 13 Processing time for different functions and kernels

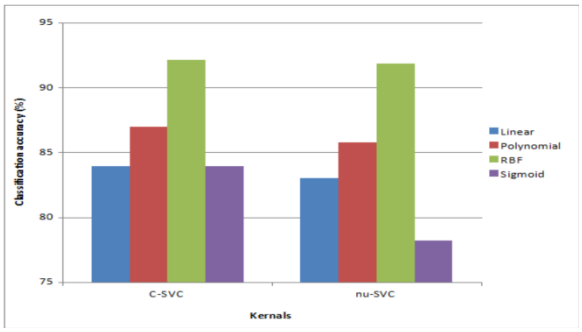

Figure 14 Classification accuracy for different functions and kernels

When all 8 methods were compared the CSVC kernel with RBF function topped the list with classification accuracy on 92.12% and processing time of 14seconds. Followed by RBF function of the nu-SVC kernel with classification accuracy of 91.82 % and processing time of 7 seconds. The analysis reports of both the functions are mentioned below. The summary of the variables used are displayed in Table 6.18.

4.1. C -SVC Classification Parameters (RBF)

Table 9 displays the SVM parameters for the Radial Basis Function with the C-SVC kernel. Table 10 displays the training dataset result for the selected function with the kernel. Table 11 displays the testing/validation dataset result for the selected function with the kernel. Table 12 displays the confusion matrix for the training data set. Table 13 displays the confusion matrix for the testing/ validation data set

Table 9 SVM parameters

Parameter	Value/ Action
Type of SVM model	C-SVC
SVM kernel function	Radial Basis Function (RBF)
Search criterion	Minimize total error
Number of points evaluated during search	132
Minimum error found by search	0.075
Epsilon	0.001
Gamma	15.02
C	451.60
Number of support vectors used by the model	115

Table 10 Training data result

Actual			Misclassified			
Category	Count	Weight	Count	Weight	Percent	Cost
NORMAL	110	110	0	0	0.00	0.00
PUNCTURE	110	110	0	0	0.00	0.00
IDLE	110	110	0	0	0.00	0.00
Total	330	330	0	0	0.00	0.00
Overall accuracy = 100%						

Table 11 Testing/Validation data result

Actual			Misclassified			
Category	Count	Weight	Count	Weight	Percent	Cost
NORMAL	110	110	12	12	10.90	0.109
PUNCTURE	110	110	14	14	12.72	0.127
IDLE	110	110	0	0	0.000	0.000
Total	330	330	26	26	7.87	0.079
Overall accuracy = 92.12%						

Table 12 Training data confusion matrix

Classified as	Normal	puncture	idle
Normal	110	0	0
Puncture	0	110	0
Idle	0	0	110

Table 13 Testing/Validation data confusion matrix

Classified as	Normal	puncture	idle
Normal	98	9	3
Puncture	12	96	2
Idle	0	0	110

A total of 115 Support Vectors were used to build the SVM model (Table 6.21). The computational time required to build the model was 14 seconds (Table 6.20 and Figure 6.17). From the confusion matrix (Table 6.24) which is generated during the training phase of the algorithm it can clearly be noted that the algorithm has achieved an impressive 100% classification accuracy. However when the trained algorithm was validated it scored a classification accuracy of 92.12% (Table 6.25). It can be noted that 98/110 samples were correctly classified as normal, 96/110 samples were correctly classified as puncture, and 110/110 samples were correctly classified as idle. The classifier achieved a maximum classification accuracy of 92.12% after training.

4.2. NU-SVC PARAMETERS (RBF)

Table 14 displays the SVM parameters for the selected function with the kernel. Table 15 displays the training dataset result for the selected function with the kernel. Table 16 displays the testing/validation dataset result for the selected function with the kernel. Table 17 displays the confusion matrix for the training data set. Table 18 displays the confusion matrix for the testing/ validation data set

Table 14 SVM parameters

Parameter	Value/ Action
Type of SVM model	Nu-SVC
SVM kernel function	Radial Basis Function (RBF)
Search criterion	Minimize total error
Number of points evaluated during search	149
Minimum error found by search	0.078
Epsilon	0.001
Nu	0.012
Number of support vectors used by the model	110

Table 15 Training data result

Actual			Misclassified			
Category	**Count**	**Weight**	**Count**	**Weight**	**Percent**	**Cost**
NORMAL	110	110	0	0	0.00	0.00
PUNCTURE	110	110	0	0	0.00	0.00
IDLE	110	110	0	0	0.00	0.00
Total	330	330	0	0	0.00	0.00
Overall accuracy = 100%						

Table 16 Testing/Validation data result

Actual			Misclassified			
Category	**Count**	**Weight**	**Count**	**Weight**	**Percent**	**Cost**
NORMAL	110	110	12	12	10.90	0.109
PUNCTURE	110	110	15	15	13.63	0.136
IDLE	110	110	0	0	0.00	0.00
Total	330	330	27	27	13.63	0.082
Overall accuracy = 91.82%						

Table 17 Training data confusion matrix

Classified as	**Normal**	**puncture**	**idle**
Normal	110	0	0
Puncture	0	110	0
Idle	0	0	110

Table 18 Testing/Validation data confusion matrix

Classified as	**Normal**	**puncture**	**idle**
Normal	98	8	4
Puncture	13	95	2
Idle	0	0	110

A total of 115 Support Vectors were used to build Table 14. The computational time required to build the model was 7 seconds (Table 8 and Figure 13). From the confusion matrix (Table 17) which is generated during the training phase of the algorithm it can be noted that the algorithm has achieved an impressive 100% classification accuracy. However when the trained algorithm was validated it scored a classification accuracy of 92.12% (Table 18). It can be noted that 98/110 samples were correctly classified as normal, 95/110 samples were correctly classified as puncture, and 110/110 samples were correctly classified as idle. The classifier achieved a maximum classification accuracy as 91.82% after training.

5. Conclusion

A safety of driver and passengers are important, monitoring automobile tyre pressure can help reduce risks of accidents related to tyres. The system acts as an early warning system there by providing sufficient time for the driver to take action. This paper proposed a new indirect method to monitor the tyre pressure by harvesting the vertical vibrations from the wheel hub of a running vehicle. A sampling frequency was chosen and the vibration signals were acquired. Since the problem was treated as a fault diagnosis problem the vibration signals were represented as histogram features. Support vector machine based algorithms were used to achieve good classification accuracy. A total of eight results were obtained (Table 7) out of which CSVC kernel with RBF function topped the list with classification accuracy of 92.12% and processing time of 14 seconds.

Reference

[1] Craighead I. A. "Sensing tyre pressure, damper condition and wheel balance from vibration measurements", Proceedings of institution of mechanical engineers Vol. 211 No. 4 Part D, pp: 257 - 265. April 1997

[2] The Royal Society for the Prevention of Accidents (RoSPA). Road safety information, *http://www.rospa.com/road-safety/advice/vehicles/tyre-safety-technology/pressure-monitoring-systems/*. January 2001.

[3] Changzheng Wei, Wei Zhou, Quan Wang, Xiaoyuan Xia and Xinxin Li.(2012)., "TPMS (tire-pressure monitoring system) sensors: Monolithic integration of surface-micro-machined piezoresistive pressure sensor and self-testable accelerometer", Microelectronic Engineering, Vol. 91, pp: 167–173, March 2012

[4] Sankaranarayanan velupillai and levent güvenç. Tire Pressure Monitoring. ,*IEEE control systems magazine*, IEEE, Vol. 1, No.1 pp: 275 to 280. December 2007.

[5] NIRA Dynamics AB and Dunlop Tech GmbH. Indirect Tire Pressure Monitoring Systems - Myths and Facts, *http://www.businesswire. com/news/ home /20120720005231/en/Nira-Dynamics-Indirect-Tire-Pressure-Monitoring-Systems #.VRUBp47ANhk*, July 2012.

[6] NIRA DYNAMICS. TPI –Advanced Indirect Tire Pressure Monitoring, NIRA Dynamics AB, *www.niradynamics.se/scripts/ resource.* April 2005

[7] Zhou Yulan, ZangYanhong and Lin Yahong. Based on Multi-sensor Information Fusion Algorithm of TPMS Research, 2012 International Conference on Solid State Devices and Materials Science, Physics Procedia Vol. 25 pp: 786 – 792. April 2012.

[8] Kanwar Bharat Singh, VishwasBedekar, Saied Taheri and ShashankPriya. Piezoelectric vibration energy harvesting system with an adaptive frequency tuning mechanism for intelligent tires, *Mechatronics*,Vol.22 pp: 970–988. October 2012.

[9] Hamed. M, B. Tesfa, M. Aliwan, G. Li,F.Gu and A.D. Ball. The Influence of Vehicle Tyres Pressure on the Suspension System Response by Applying the Time-Frequency Approach, International Conference on Automation & Computing, Brunel University, London, UK, pp: 1 - 6. September 2013.

[10] Carcaterran. A and N.Roveri. Tire grip identification based on strain information: Theory and simulations, *Mechanical Systems and Signal Processing*, Vol. 41, No.1 -2, pp: 564 - 580. June 2013.

[11] Dubois. G, J. Cesbron, H.P. Yin, F. Anfosso-Lédée and D. Duhamel. Statistical estimation of low frequency tyre/road noise from numerical contact forces, *Applied Acoustics*, Vol.74, pp: 1085–1093. March 2013.

[12] Amarnath. M, V. Sugumaran and Hemantha Kumar. Exploiting sound signals for fault diagnosis of bearings using decision tree, *Measurement*, Vol. 46, pp: 1250–1256. April 2013.

[13] Jegadeeshwaran. R and V. Sugumaran. Comparative study of decision tree classifier and best first tree classifier for fault diagnosis of automobile hydraulic brake system using statistical features, *measurement*, Vol. 46, No. 9, pp: 3247 - 3260. November 2013.

[14] Muralidharan. V and V. Sugumaran. Feature extraction using wavelets and classification through decision tree algorithm for fault diagnosis of mono-block centrifugal pump, *Measurement*, Vol. 46, pp: 353–359. January 2013.

[15] Muralidharan. V and V. Sugumaran. Rough Set Based Rule Learning and Fuzzy Classification of Wavelet Features for Fault Diagnosis of Monoblock Centrifugal Pump, *International measurement confederation*, Vol. 46, No. 9, pp: 3057 - 3063. November 2013.

[16] Quinlan, R. Improved use of continuous attributes in C45. Journal of Artificial Research, Vol. 4, pp: 77–90. March1996

[17] Babu Devasenapati, V. Sugumaran and K.I. Ramachandran. Misfire identification in a four-stroke four-cylinder petrol engine using decision tree, Expert Systems with Applications, Vol. 37, pp: 2150–2160. March 2010.

[18] Muralidharan. V, V. Sugumaran and . Fault Diagnosis of Monoblock Centrifugal Pump using SVM, *Engineering Science and Technology, an International Journal*, Vol. 17, No. 3, pp: 152-157. September 2014.

Author biography

Hemanth Mithun Praveen was born in Trivandrum, Kerala, in 1991. He completed his B.E in mechanical engineering from Noorul Islam university, Thuckalay, kanyakumari district, Tamil nadu in the year 2013. At present he is pursuing his M.S by research at VIT University, Chennai, Tamil Nadu, India. His research is in the field of fault diagnosis.

Dr. V. Sugumaran received the B.E. degree in Mechanical Engineering from the Amrita Institute of Technology & Science, 1998 and the M.Tech in Production Engineering, from The National Institute of Engineering, 2003. Ph.D. degree in Fault Diagnosis, from Amrita School of Engineering, Amrita University, Coimbtore, Tamil Nadu, India, in 2008. From 2000 to 2009, he was an Associate Professor, with the Amrita School of Engineering, Coimbatore, Tamil Nadu. From 2009 t0 2011, he was working with SRM University, Chennai, Tamil Nadu. Since 2011, he has been an Associate Professor with the School of Mechanical and Building Sciences, VIT University, Chennai, Tamil Nadu, India. He is the author of two books, more than 85 international journal publications. He has also filed three patents. His research interests include Condition Monitoring & Fault Diagnosis, Machine learning / Data mining in manufacturing and Mechanical Engineering. He presented papers in 43 International / National Conferences. He is also acting as a Reviewer for many international journals and editor for four international journals.